Available online at www.sciencedirect.com
SCIENCE DIRECT
Trans. Nonferrous Met. Soc. China 18(2008) 1058−1064
Transactions of Nonferrous Metals Society of China
www.csu.edu.cn/ysxb/

Effect of combinative addition of strontium and rare earth elements on corrosion resistance of AZ91D magnesium alloy

NIU Jie-xin(钮洁欣), CHEN Qiu-rong(陈秋荣), XU Nai-xin(徐乃欣), WEI Zhong-ling(卫中领)

Shanghai Institute of Microsystem and Information Technology, Chinese Academy of Sciences, Shanghai 200050, China

Received 22 January 2008; accepted 4 May 2008

Abstract: The influence of strontium(Sr) and rare earth(RE) elements on the corrosion behavior of AZ91D magnesium alloy was investigated by conventional corrosion testing and electrochemical measurements in 3.5% NaCl solution. After comparing the mass loss and hydrogen evolution of the samples, the microstructures of the alloys and the morphologies of their corrosion product films were characterized by electron probe microanalysis-energy dispersive spectrometry(EPMA-EDS) and Auger electron spectroscopy(AES). Compared with individual addition of Sr or RE to AZ91D, the combinative addition of 0.5% Sr and 1% RE to AZ91D successfully decreases the corrosion rate further, which can be attributed to the depression of micro-galvanic couples, as well as the formation of more protective film due to aluminum enrichment. The combinative addition of strontium and rare earth elements to AZ91D magnesium alloy appears to be a promising approach to increase its corrosion resistance.

Key words: strontium; rare earth elements; AZ91D alloy; corrosion; microstructure

1 Introduction

Fulfilling the role admirably as ‘ultra light’ alloys, magnesium alloys have wide applications in portable sectors. However, their extreme susceptibility to corrosion in comparison with other metals has greatly limited further utilization. Previous studies[1−4] showed that for magnesium alloys, rare earth(RE) elements have distinguished feature of corrosion resistance enhancement.

The advantage of RE in magnesium alloy is attributed to trapping deleterious elements. FAN et al[5] considered that the addition of cerium, a typical RE element, prompts the formation of Al- enriched layer on the corrosion film, which contributes to the corrosion resistance of AZ91D alloy.

Also, other researches[6−10] indicated that the addition of alkaline earth elements, especially calcium (Ca) and strontium(Sr), to magnesium alloys could improve mechanical properties because of grain refinement.

YOU et al[11] believed that the oxidation of magnesium at elevated temperature could be retarded by Ca addition to magnesium alloys. The oxide layer of Mg-Ca alloys was much thinner and more compact than that of pure magnesium, which could be attributed to the MgO/CaO protective layer formed at elevated temperature. Recently, WU et al[12] reported that the addition of 1% Ca and 1% RE to AZ91 alloy caused the decrease of corrosion rate to 19.0% that of AZ91 alloy. The improvement was attributed to the formation of reticular Al_2Ca acting as a barrier against corrosion.

As previously mentioned, the alkaline earth element, calcium, has some positive effects, such as improvement of oxide film property and prevention of further corrosion, on magnesium alloys besides rare earth elements. Nevertheless, there are little reports on the effect of another alkaline earth element, strontium, on the corrosion performance[13−14]. And to our knowledge, the role of combinative addition of Sr and RE on the corrosion resistance of magnesium alloys has not been systematically investigated, which would be certainly more interesting to explore. AZ91D (Mg-9Al-1Zn) is one of the most popular commercial magnesium alloys, whose corrosion rate is relatively lower than that of other Mg-Al alloys. In this work, the influence of both Sr and

Foundation item: Project(065211030) supported by Municipal Science and Technology Commission of Shanghai, China
Corresponding author: NIU Jie-xin; Tel: +86−21−6251070−8966; E-mail: nutirtion1@126.com

RE (especially cerium-enriched) on the corrosion behavior of AZ91D magnesium alloys was investigated by conventional corrosion testing and electrochemical measurements. The microstructures of the alloys and the morphologies of their corrosion product films were also characterized to understand the role of Sr and RE addition.

2 Experimental

Magnesium alloys were firstly melted in a crucible furnace under the shelter of CO_2+SF_6 gases and cast in a water-cooled metallic mould by gravity casting process. Then appropriate amounts of strontium (99.9% in purity) and mixed rare earth (cerium-enriched) elements were added into the molten AZ91D alloys. The actual compositions of the alloys for study were determined by inductively coupled plasma-atomic emission spectrometry (ICP-AES) analysis and the results are presented in Table 1 with specific alloy code listed.

The specimens for general corrosion tests were in the dimensions of 14 mm × 14 mm × 4 mm. The specimens for electrochemical measurements were embedded in epoxy resin with one side exposed (1 cm^2) as working surface. All samples were ground with 1000 grit SiC paper, degreased, washed and dried before testing. The specimens for EPMA-EDS (electron probe microanalysis and energy dispersion spectrometry) and AES (Auger electron spectroscopy) were additionally polished up to 1 μm finish.

As the corrosion products of magnesium alloys in NaCl solution always contain $Mg(OH)_2$, most tests were carried out in 3.5% NaCl solution with saturated $Mg(OH)_2$, which is the common corrosion medium in many literatures[6, 15−16]. The temperature of the solution was maintained at 25 ℃ during the experiments.

Two representative data, mass loss and hydrogen evolution, were finally measured to evaluate corrosion rate of the alloys. The electrochemical measurements were carried out in a three-electrode (saturated calomel electrode as a reference, with a platinum electrode as counter and a sample as the working electrode) cell containing 500 mL test solution by using CHI604b electrochemical measurement system. For potentio-dynamic polarization curves the potential scanning started from −1 750 mV (vs SCE) and stopped at −1 400 mV (vs SCE) with scanning rate of 0.167 mV/s. The microstructures and the corrosion products of the alloys were characterized by EPMA-EDS analysis. The transition of composition across the oxide layer and metal surface was investigated by AES using VG Scientific Microlab 310F Field Emission Scanning Auger Microprobe with electron beam energy of 10 keV and beam current of 4.5 nA (measured by Faraday cup). Argon ion sputtering was carried out using an ion beam energy of 3 keV, a beam current of 0.23 nA and a raster area of 0.24 mm^2.

3 Results and discussion

3.1 Effect of combinative addition of Sr and RE on corrosion rate of AZ91D alloys

The element Fe in magnesium alloys is found to have severe degradation effects. Even trace of Fe will lead to poor reputation of magnesium for saltwater corrosion durability[17]. However, this degradation effect could be suppressed by the element Mn. MAKAR et al[18] indicated that the corrosion resistance of magnesium alloys could be greatly improved when the Fe/Mn ratio in the alloys is below 0.032. All the alloys of the present research are added with 0.1%−0.2% Mn, which efficiently keeps the Fe/Mn ratio in the range of 0.01−0.02. Thus, their corrosion resistance is better than that of commercially available AZ91D alloys. This research is mainly focused on the effect of combinative addition of Sr and RE to further improve the corrosion resistance of magnesium alloys.

Fig.1 shows the average corrosion rates obtained from mass loss of AZ91D alloys with single addition of RE or Sr immersed in 3.5% NaCl solution with saturated $Mg(OH)_2$ for 24 h. Appropriate amount of individual RE

Table 1 Chemical composition of magnesium alloys (mass fraction, %)

Alloy	Al	Sr	Ce	La	Mn	Zn	Fe	Mg
Mg-9Al(AZ91D)	9.01	−	−	−	0.17	0.75	＜0.002	Bal.
Mg-9Al-1RE(AZR1)	8.59	−	0.39	0.22	0.11	0.68	＜0.002	Bal.
Mg-9Al-2RE(AZR2)	8.61	−	0.70	0.40	0.11	0.71	＜0.002	Bal.
Mg-9Al-0.3Sr(AZS0.3)	9.16	0.32	−	−	0.20	0.74	＜0.002	Bal.
Mg-9Al-0.6Sr(AZS0.6)	8.74	0.61	−	−	0.18	0.69	＜0.002	Bal.
Mg-9Al-1.4Sr(AZS1.4)	8.64	1.37	−	−	0.17	0.72	＜0.002	Bal.
Mg-9Al-1RE-0.5Sr(AZRS0.5)	8.51	0.53	0.42	0.28	0.10	0.72	＜0.002	Bal.
Mg-9Al-1RE-0.8Sr(AZRS0.8)	8.82	0.84	0.43	0.32	0.11	0.72	＜0.002	Bal.

or Sr would improve the corrosion resistance of AZ91D alloy to some extent. However, excessive Sr or RE addition leads to an increase of the corrosion rate, which could be attributed to more severe inhomogeneity due to additionally precipitated phases. Moreover, it is noticed that the corrosion rate of AZ91D alloy can be further reduced by combinative addition of Sr and RE, which is more effective for enhancing the corrosion resistance of AZ91D alloys than single addition of Sr or RE. Especially for the case of 1%RE and 0.5% Sr, as shown in Fig.2, the corrosion rate is decreased by 54.3%, in comparison with that of AZ91D alloy.

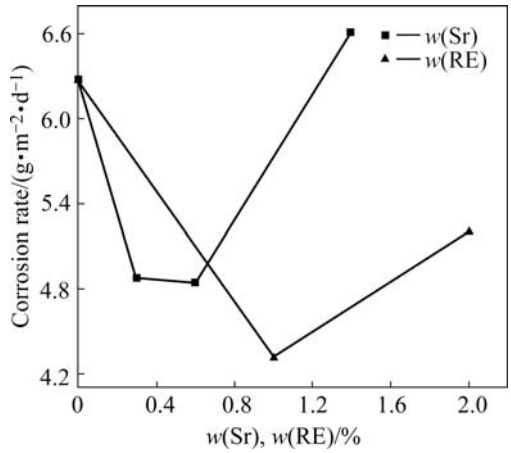

Fig.1 Average corrosion rates from mass loss in 24 h for Mg-9Al alloys by single addition of Sr or RE in 3.5% NaCl solution with saturated $Mg(OH)_2$ at pH 10.5 and 25 ℃

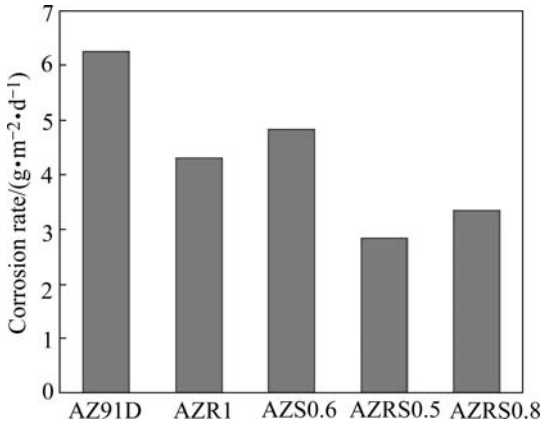

Fig.2 Average corrosion rates from mass loss in 24 h for AZ91D, AZR1, AZS0.6, AZRS0.5 and AZRS0.8 alloys in 3.5% NaCl solution with saturated $Mg(OH)_2$ at pH 10.5 and 25 ℃

The corrosion rate can also be assessed by hydrogen evolution (with hydrogen evolution rate of 0.01 mL/(cm·h) equal to current density of 2.39×10^{-5} A/cm^2 according to the Faraday's law), which shows instantaneous corrosion rates and enables us to trace its change with time. Fig.3 illustrates that the hydrogen evolution rate of the RE-contained or Sr-contained alloys is significantly less than that of AZ91D alloy. And the hydrogen evolution rate of AZRS0.5 alloy due to the combinative addition of Sr and RE is always the lowest at any time in 24 h. The variation tendency is consistent with that of mass loss measurements.

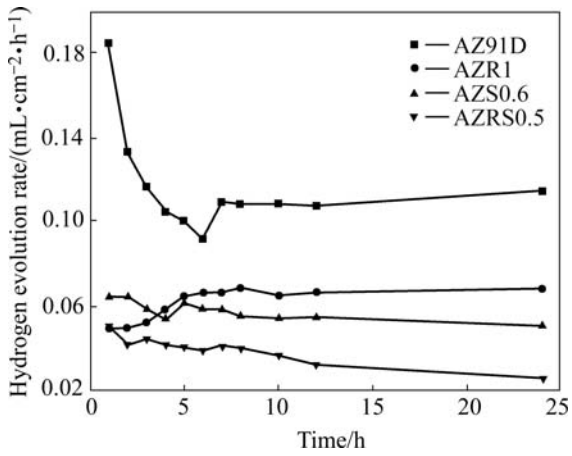

Fig.3 Hydrogen evolution rates for AZ91D, AZR1, AZS0.6 and AZRS0.5 alloys in 3.5% NaCl solution with saturated $Mg(OH)_2$ at pH 10.5 and 25 ℃

The above results indicate that the effect of combinative RE and Sr addition to AZ91D alloys is more significant than that of their single addition.

3.2 Effect of combinative addition of RE and Sr on microstructure of AZ91D alloys

The microstructures of AZ91D alloys, including the content and distribution of phase, the grain shape and the grain size, vary with RE and Sr addition and influence the corrosion behavior of the alloys. Fig.4 illustrates the microstructures of four different alloys by EPMA analysis. The microstructure of AZ91D magnesium alloy consists of α-Mg matrix and β-$Mg_{17}Al_{12}$ phase particles, which precipitate along grain boundaries[19]. There are also a few brighter block-like Mn-contained phases in Mg matrix due to the presence of Mn as alloying element. Single addition of RE or Sr changes the microstructure of AZ91D alloys. Some new rod-like and cosh-like intermetallic phases appear and the amount of β-$Mg_{17}Al_{12}$ phase apparently decreases and its distribution becomes discontinuous. With combinative addition of 0.5% Sr and 1% RE, the β-$Mg_{17}Al_{12}$ phase is dispersed and other exiguous phases irregularly precipitate in α phase and around β-$Mg_{17}Al_{12}$ phase (shown in Fig.5). These phases with various shapes are RE-rich or Sr-rich phases, whose compositions are presented in Table 2.

The corrosion of magnesium alloys is related to the difference of electrode potentials in different parts of magnesium alloys, which results in micro-galvanic couples. As reported, the potential of β-$Mg_{17}Al_{12}$ phase is −1.20 V (vs SCE), more positive than that of α-Mg

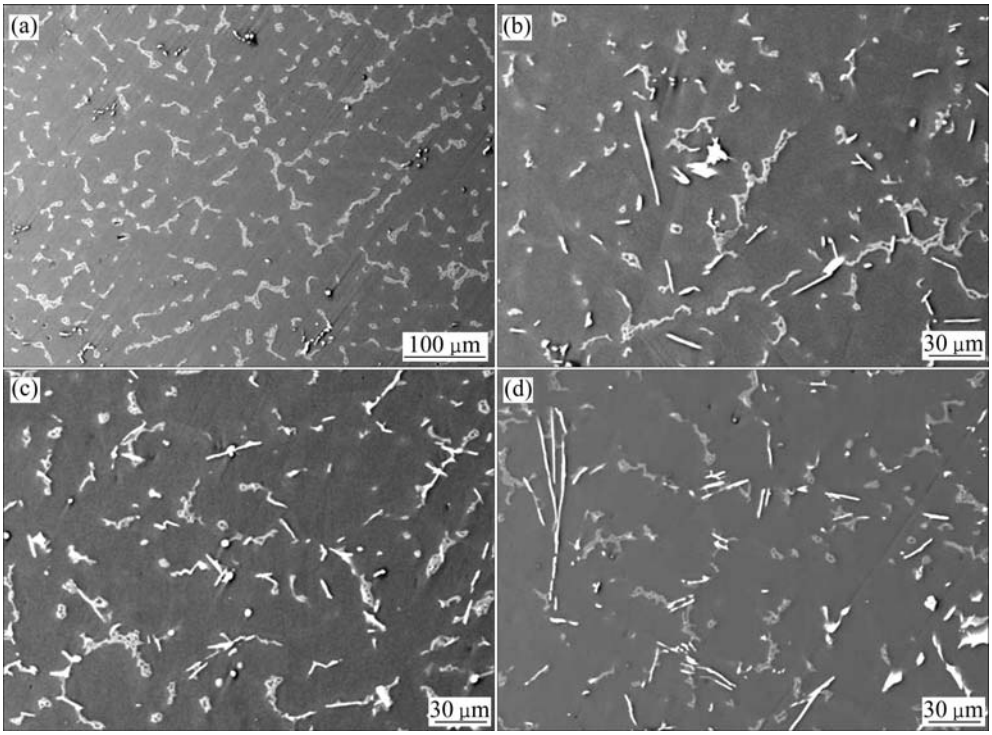

Fig.4 EPMA micrographs of AZ91D (a), AZR1 (b), AZS0.6 (c) and AZRS0.5 (d) alloys

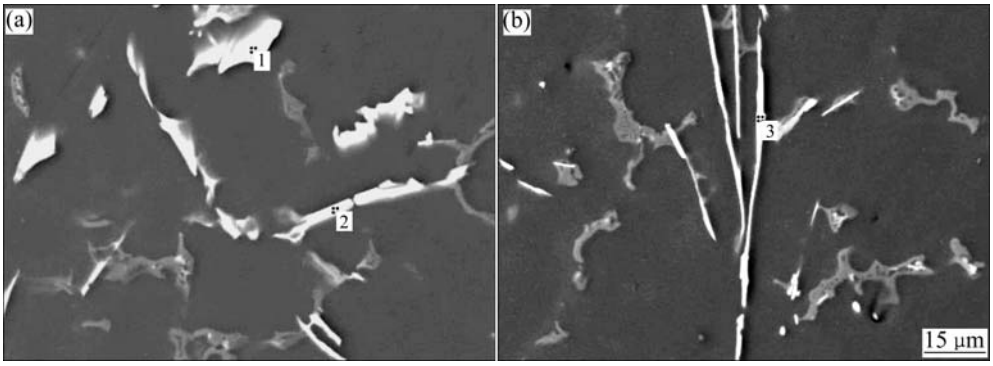

Fig.5 EPMA micrograph of AZRS0.5 alloy

Table 2 Chemical composition of various phases in AZRS0.5 alloy (mass fraction, %)

Analysis area	Mg	Al	Ce	La	Nd	Sr
1 (MgAlRE phase)	19.66	33.08	26.99	15.88	4.40	−
2 (MgAlRE phase)	36.75	25.96	21.63	10.67	5.00	−
3 (MgAlRESr phase)	29.05	30.17	20.37	12.61	4.95	2.85

(−1.66 V (vs SCE))[20]. These two phases form a micro-galvanic couple, α-Mg phase as anode while β-$Mg_{17}Al_{12}$ phase as cathode. For this study the intermetallic compounds of Mg-Al-RE and Mg-Al-Sr were specially prepared to simulate the RE-contained phase and Sr-contained phase in AZ91D alloys. Their open circuit potentials are listed in Table 3. The electrode potential of intermetallic compounds 50Mg-30Al-10RE and 70Mg-24Al-6Sr is more negative than that of β-$Mg_{17}Al_{12}$ phase, which indicates that their cathodic effect is weaker than that of β-$Mg_{17}Al_{12}$ phase in the couple and the drive of the couple is diminished. Hence, their appearance is beneficial to depressing the micro-galvanic effect.

The relative ratio of phase distribution in AZ91D alloys is also taken into consideration. EPMA analysis based on the different colors of different phases provided information on the α-Mg and β-$Mg_{17}Al_{12}$ phase fraction

in the alloy. The fraction of each phase was then calculated according to the pixel size. The results are listed in Table 4. Compared with AZ91D alloy, the fraction of β-$Mg_{17}Al_{12}$ phase in AZR1 and AZS0.6 alloys decreases as a result of the addition of RE or Sr. The RE-contained or Sr-contained phases (marked as "RS-phases") appear to act as additional cathodes. However, the addition of RE and Sr reduces the total cathode fraction. For AZRS0.5 alloy, the fraction of cathode phases is the least among the four alloys studied. Since the corrosion of AZ91D alloys is controlled by cathodic polarization, the reduction of cathode components helps to weaken cathodic effect and depress the micro-galvanic corrosion of magnesium alloys.

Table 3 Open circuit potentials of specifically prepared inter-metallic phases in 3.5% NaCl solution at pH 10.5 and 25 ℃

Nominal phase composition	Open circuit potential (vs SCE)/V
α-Mg phase	−1.66
β-$Mg_{17}Al_{12}$ phase	−1.20
50Mg-30Al-10RE	−1.414
70Mg-24Al-6Sr	−1.406

Table 4 Fraction of α-phase, β-phase and RS-phase in Mg-9Al alloys (%)

Alloy	α-phase	β-phase	RS-phase	β-phase+ RS-phase
AZ91D	91.8	8.2	0	8.2
AZR1	93.0	5.4	1.5	6.9
AZS0.6	93.0	4.6	2.4	7.0
AZRS0.5	95.0	2.7	2.4	5.0

3.3 Effect of combinative addition of Sr and RE on electrochemical behavior of AZ91D alloys

Fig.6 presents the potentiodynamic polarization curves of the four magnesium alloys. Firstly the cathodic polarization curves of AZR1 alloy and AZS0.6 alloy are not as steep as that of AZ91D alloy. This implies that the cathodic process of Mg-9Al-1Zn alloy is relaxed to some extent. The cathodic polarization curve of AZRS0.5 alloy is further flat. Secondly, as listed in Table 5, the corrosion current density deduced from polarization measurements could be ranked in the following order: AZ91D > AZS0.6 > AZR1 > AZRS0.5. This result is approximately in accordance with the above mentioned corrosion rate measurements. Thirdly, the anodic polarization curves show an anodic current plateau, i.e. anodic breakthrough, which verifies the presence of a protective film on the alloy. The length of the anodic current plateau of AZRS0.5 alloy is about 60 mV, twice that of AZR1 alloy (about 30 mV), which indicates that AZRS0.5 alloy has more protective layer on surface.

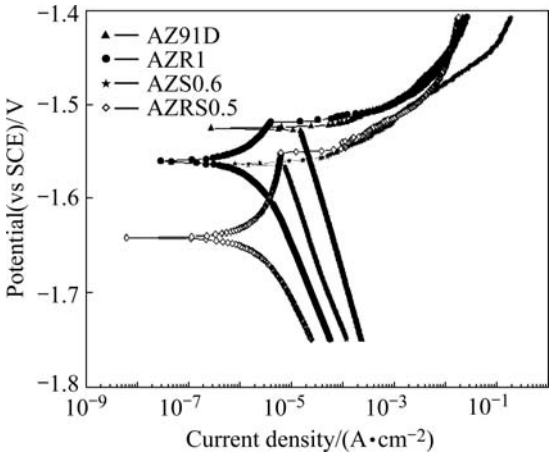

Fig.6 Polarization curves of AZ91D, AZR1, AZS0.6 and AZRS0.5 alloys in 3.5% NaCl solution with saturated $Mg(OH)_2$ at pH 10.5 and 25 ℃

Table 5 Corrosion potentials and corrosion current densities of AZ91D, AZR1, AZS0.6 and AZRS0.5 alloys in 3.5% NaCl solution with saturated $Mg(OH)_2$ at pH 10.5 and 25 ℃

Alloy	J_{corr}/(μA·cm^{-2})	φ_{corr} (vs SCE)/V
AZ91D	16.85	−1.52
AZR1	2.37	−1.56
AZS0.6	6.75	−1.56
AZRS0.5	2.01	−1.64

3.4 Effect of combinative addition of Sr and RE on corrosion product films of AZ91D alloys

Corrosion product film on alloy usually makes great contributions to its corrosion resistance. Dense and compact film provides satisfactory protection. In our study, 2 h immersion in 3.5% NaCl solution with saturated $Mg(OH)_2$ was selected to get the corrosion product film. The elemental state and distribution of the corrosion film of four different alloys were investigated after the immersion.

Fig.7 shows the Auger depth profiles of four different alloys for oxygen and aluminum elements. The Sr and RE elements can not be measured because of the detection precision of the instrument. Oxygen concentration gradually decreases with film depth, which shows the presence of an outer oxide layer on the surface. The decreasing rate of oxygen concentration can be ranked as: AZRS0.5 > AZR1 > AZ91D > AZS0.6. The elevated aluminum concentration shows the presence of an Al-enriched layer on the surface of the alloys with individual RE or Sr addition, especially with Sr addition. For AZ91D alloy, aluminum concentration always retains a low level and fluctuates, indicating the absence of similar Al-rich layer. In this case, the main component in corrosion product film is magnesium oxide, which is unstable and easily forms hydroxide in NaCl solution,

resulting in reduced corrosion resistance of AZ91D alloys. The film containing aluminum oxide is more dense and compact than magnesium oxide, and thus becomes a barrier to further corrosion[21]. Moreover, owing to the combined action of RE and Al, the Mg-Al composite oxide on the Mg-Al alloy surface can hardly form hydroxide, which helps to maintain the integrality of the oxide layer and consequently improves the corrosion resistance[22].

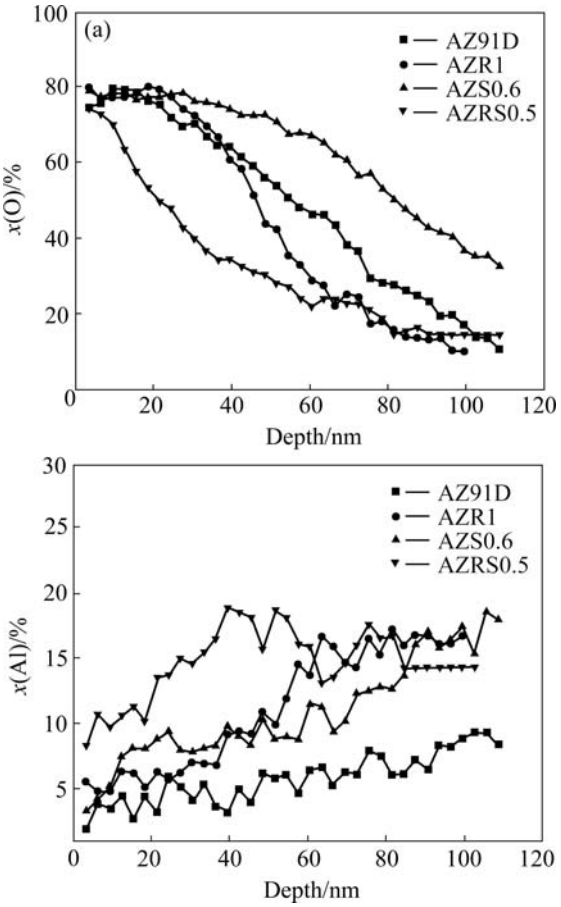

Fig.7 Auger depth profiles for oxygen and aluminum elements of AZ91D, AZR1, AZS0.6 and AZRS0.5 alloys after immersion in 3.5% NaCl solution with saturated $Mg(OH)_2$ for 2 h

As for AZRS0.5 alloy, the aluminum concentration in corrosion film is the highest among the four alloys. Moreover, oxygen concentration is quite high at the first stage of sputtering and then dramatically decreases with further sputtering. So, the oxygen concentration in the inner layer is much lower, which demonstrates that there is a quite thin oxide layer on the outer layer with good protection performance. These effects contribute to the enhanced corrosion resistance of AZ91D alloys and restrain the corrosion of magnesium alloy.

Three-dimensional Auger electron spectra(AES) of the four alloys can provide further information on the film. A typical spectrum is illustrated in Fig.8. When the surface film is stripped, the peaks for Mg shift to lower kinetic energy and fine structure appears, which correspond to the transformation of chemical structure of magnesium atoms from Mg—O bonding to Mg—Mg bonding. Such transformation takes place at the boundary between magnesium and its oxide, which can be used as an index to identify the thickness of oxide layer. For AZ91D alloy, the fine structures of Mg peaks are observed after 24-level sputtering (about 3 nm thick per level), which implies that the thickness of oxide layer for AZ91D alloy is about 70 nm. The thickness of the oxide magnesium layer of four alloys is listed in Table 6, which can be ranked from thin to thick as: AZ91D, AZS0.6, AZR1 and AZRS0.5. This is in accordance with the above results, indicating that the corrosion rate of

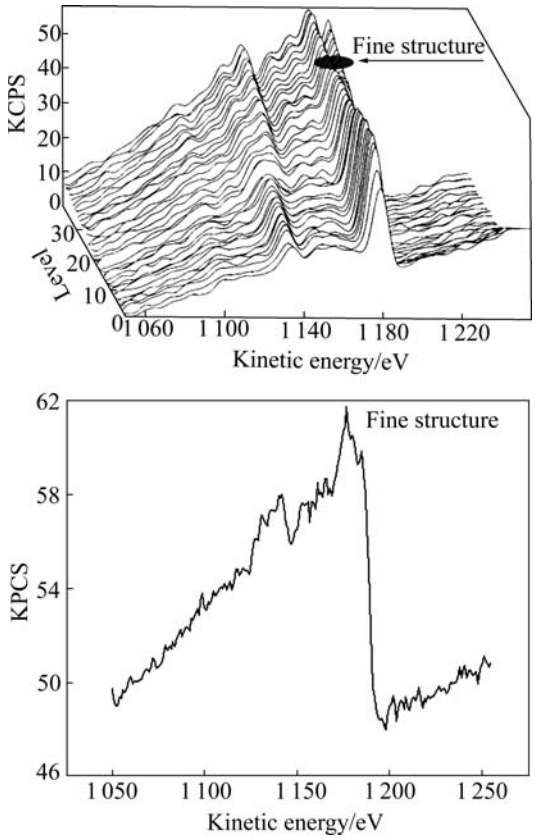

Fig.8 Three-dimensional Auger electron spectra of AZ91D alloys after immersion in 3.5% NaCl solution with saturated $Mg(OH)_2$ for 2 h

Table 6 Thickness of oxide magnesium layer of AZ91D, AZR1, AZS0.6 and AZRS0.5 alloys after immersion in 3.5% NaCl solution with saturated $Mg(OH)_2$ for 2 h

Alloy	Sputtering level of magnesium oxide layer	Thickness of magnesium oxide layer/nm
AZ91D	24	72
AZS0.6	23	69
AZR1	11	33
AZRS0.5	7	21

magnesium alloys is dominated by the density.

4 Conclusions

1) The effect of combinative Sr and RE addition on corrosion resistance of AZ91D alloys is more significant than that of their single addition. With 1%RE and 0.5% Sr addition, the corrosion rate of AZ91D alloy decreases by 54.3%.

2) The combinative Sr and RE addition to Mg-9Al-1Zn alloys has beneficial effect on refining and decomposing of β-$Mg_{17}Al_{12}$ phase. This weakens the cathodic role of β-$Mg_{17}Al_{12}$ phase and efficiently depresses the micro-galvanic couple so as to reduce the corrosion.

3) The synergic effect of RE and Sr makes the corrosion product film more protective. The formed Al-enriched layer is stable and keeps intact in the media containing Cl^-, which contributes to the enhanced corrosion resistance of AZ91D alloy.

Acknowledgements

The authors would like to thank Prof. HUANG Yuan-wei, Prof. ZHANG Chen-dian, Mrs. DING Cui-hong, Dr. ZHANG Ya, Dr. ZHOU Xue-hua and Mr. HU Shao-feng for their help during the investigation. The authors are also indebted to the Corrosion Research Center of Shanghai Institute of Microsystem and Information Technology, Chinese Academy of Sciences, for the experimental facilities and financial support.

References

[1] SONG G L, STJOHN D. The effect of zirconium grain refinement on the corrosion behaviour of magnesium-rare earth alloy MEZ [J]. Journal of Light Metals, 2002, 2(1): 1−16.

[2] TAKENAKA T, ONO T, NARAZAKI Y, NAKA Y, KAWAKAMI M. Improvement of corrosion resistance of magnesium metal by rare earth elements [J]. Electrochimica Acta, 2007, 53(1): 117−121.

[3] NORDLIEN J H, NISANCIOGLU K, ONO S, MASUKO N. Morphology and structure of water-formed oxides on ternary MgAl alloys [J]. Journal of the Electrochemical Society, 1997, 144(2): 461−466.

[4] ROSALBINO F, ANGELINI E, DE NEGRI S, SACCONE A, DELWNO S. Effect of erbium addition on the corrosion behaviour of Mg-Al alloys [J]. Intermetallics, 2005, 13(1): 55−60.

[5] FAN Yu, WU Guo-hua, ZHAI Chun-quan. Influence of cerium on the microstructure, mechanical properties and corrosion resistance of magnesium alloy [J]. Materials Science and Engineering A, 2006, 433(1/2): 208−215.

[6] BEN-HAMU G, ELIEZER D, SHIN K S. The role of Si and Ca on new wrought Mg-Zn-Mn based alloy [J]. Materials Science and Engineering A, 2007, 447(1/2): 35−43.

[7] QIAN Bao-guang, GENG Hao-ran, TAO Zhen-dong, ZHAO Peng, TIAN Xian-fa. Effects of Ca addition on microstructure and properties of AZ63 magnesium alloy [J]. Trans Nonferrous Met Soc China, 2004, 14(5): 987−991.

[8] POLMEAR I J. Recent developments in light alloys [J]. Materials Transations JIM, 1996, 37(1): 12−31.

[9] LIU Xiang-guo, PENG Xiao-dong, XIE Wei-dong, WEI Qun-yi. Preparation technologies and applications of strontium-magnesium master alloys [J]. Materials Science Forum, 2005, 488/489: 31−34.

[10] PEKGULERYUZ M O, BARIL E, HRYN J. Magnesium Technology [M]. New Orleans, LA, United States: TMS (The Minerals, Metals and Materials Society), 2001: 119−125.

[11] YOU B S, PARK W W, CHUNG I S. The effect of calcium additions on the oxidation behavior in magnesium alloys [J]. Scripta Materialia, 2002, 42: 1089−1094.

[12] WU Guo-hua, FAN Yu, GAO Hong-tao, ZHAI Chun-quan, ZHU Yan-ping. The effect of Ca and rare earth elements on the microstructure, mechanical properties and corrosion behavior of AZ91D [J]. Materials Science and Engineering A, 2005, 408(1/2): 255−263.

[13] KLASSEN R D, ROBERGE P R, LAFRONT A M, OTEYAKA M O, GHALI E. Corrosion behaviour of zinc and aluminum magnesium alloys by scanning reference electrode technique and electrochemical noise [J]. Canadian Metallurgical Quarterly, 2005, 44(1): 47−52.

[14] LAFRONT A M, ZHANG W, JIN S, TREMBLAY R, DUBE D, GHALI E. Pitting corrosion of AZ91D and AJ62x magnesium alloys in alkaline chloride medium using electrochemical techniques [J]. Electrochemica Acta, 2005, 51: 489−501.

[15] ZHOU Xue-hua, HUANG Yuan-wei, WEI Zhong-ling, CHEN Qiu-rong, GAN Fu-xing. Improvement of corrosion resistance of AZ91D magnesium alloy by holmium addition [J]. Corrosion Science, 2006, 48: 4223−4233.

[16] NAKATSUGAWA S, KAMADO Y, KOJIMA R, NINOMIYA K, KUBOTA K. Corrosion of magnesium alloys containing rare earth elements [J]. Corrosion Reviews, 1998, 116(1/2): 139−157.

[17] HANAWALT J D, NELSON C E, PELOUBET J A. Corrosion studies of magnesium and its alloys [J]. Transactions of the Metallurgical Society of AIME, 1942, 147: 273−299.

[18] MAKAR G L, KRUGER J. Corrosion of magnesium [J]. International Materials Reviews, 1993, 38(3): 138−153.

[19] LUNDER O, LEIN J E, AUNE T Kr, NISANCIOGLU K. Role of $Mg_{17}Al_{12}$ phase in the corrosion of Mg alloy AZ91 [J]. Corrosion, 1989, 45(9): 741−748.

[20] OTTO L, MAVIANNE V, KEMAL N. Corrosion resistant magnesium alloys [C]// 950428, Magnesium in Vehicle Design, SAE International SP-1096. 1995.

[21] LI Shi-hui, CHEN Fu-rong. A review of corrosion resistance of magnesium-aluminum-RE alloys [J]. Corrosion and Protection, 2007, 28: 333−336. (in Chinese)

[22] SONG Guang-ling, ATRENS A, WU Xian-liang, ZHANG B. Corrosion behaviour of AZ21, AZ501 and AZ91 in sodium chloride [J]. Corrosion Science, 1998, 40(10): 1769−1791.

(Edited by YANG Bing)